

Research Journal of Pharmaceutical, Biological and Chemical Sciences

Mathematical Model for Polyamide-6/Chitosan Blend Membrane Preparation.

Ayman El-gendi, Ashraf Amin*, and Heba Abdallah.

Chemical Engineering & Pilot Plant Department Engineering Research Division, National Research Center, 33 El-Bohouth St., Dokki, Cairo, Egypt, Post Code 12311.

ABSTRACT

The performance of a ternary system with one low molecular weight component, formic acid (FA) as solvent; and two high molecular weight polymers, Polyamide-6 (PA-6) and Chitosan (CS) was mathematically investigated using an extended modified Flory-Huggins model. The model predicts the volume fractions of the polymers in the membrane and coagulation bath as a function of time and membrane thickness, the Gibbs free energy of the process, and the change in chemical potential for each component. The model predictions indicated that the miscibility of PA-6 and CS blend solution was achieved for all compositions at room temperature. The volume fraction of PA-6 was varied between 0.43:0.022, resulting in a slight change of the Gibbs free energy (ΔG_m) from -3.14:-4.06 kJ/mole respectively. The predicted results from the critical temperature model for superiority properties of polymer blend solution have shown that the upper critical saturation temperature (UCST) is 323K at a PA-6 volume fraction of 0.4 and the lower critical saturation temperature (LCST) is 344K at a Chitosan volume fraction of 0.093. A diffusion model was developed to investigate the immersion/precipitation process. The diffusion model has shown that the solvent volume fraction increased with time in the coagulation bath, while the polymer volume fraction decreased owing to solvent dissolution in the coagulation bath and membrane formation.

Keywords: Model; ternary system; Immersion precipitation; Polyamide-6 membrane; Chitosan.

**Corresponding author*

INTRODUCTION

Membrane technology is widely used in different engineering applications. Permeable membrane effectively allows the transport of substances between two solutions with different concentrations [i-ii]. Variety of membranes were developed for different applications especially water treatment, such as microfiltration (MF), ultrafiltration (UF), nanofiltration (NF), reverse osmosis (RO) and membrane distillation (MD) [iii]. Membrane preparation, with repeatable and homogenous properties in laboratory environment, is highly exaggerated by several parameters such as membrane materials, variation of drawing speed, variation in retention time and water temperature variation. The membrane preparation process is complicated by the need of different thicknesses of membranes.

Phase inversion process is the most used technique to prepare both asymmetric and symmetric polymeric membranes. In addition, the morphology and performance of membranes depend on phase inversion process parameters [iv], which in turn are related to the membrane preparation process parameters. During membrane preparation, polymers and solvents are mixed in suitable ratios to form a membrane for specific applications. Due to the difficulty in studying the process parameters, modelling can be used to predict the behavior of membrane blend under different conditions. The Flory-Huggins theory [v] is found to be a convenient and useful framework for thermodynamic analysis for a membrane preparation. Phase inversion procedure can be described as a de-mixing process whereby the initially homogeneous polymer solution is transformed in a controlled manner from a liquid to a solid state [vi-vii]. The membrane production can be accomplished in several ways [viii]:

- (a) Immersion precipitation, where the polymer solution is immersed in a non-solvent such as water (coagulation bath). De-mixing and precipitation occur due to the exchange of the miscible solvent (in polymer solution) and non-solvent.
- (b) Thermally induced phase separation, this method is proposed to overcome the defects in membrane preparation when the temperature is decreased. The solvent is removed by extraction, evaporation or freeze drying.
- (c) Evaporation-induced phase separation; the polymer solution is prepared using a solvent or a mixture of a volatile non-solvent. By evaporating the solvent, the precipitation or de-mixing/precipitation takes place.
- (d) Vapor-induced phase separation; the polymer solution is exposed to an atmosphere containing a non-solvent (such as water); absorption of non-solvent causes de-mixing/precipitation.

Immersion precipitation and thermally induced phase separation are the commonly used methods in the fabrication of polymeric membranes with various morphologies [ix-x].

By varying the volume fraction of each polymer with the volume fraction of solvent over a wide range of conditions, one can study the effect of the various parameters controlling the coagulation process [xi-xii]. However, such a process will be time and material consuming process. Instead, a mathematical model can be used to predict the behavior of the polymers and the solvent in the coagulation bath [xiii]. The mathematical model will provide detailed outcomes of the coagulation process, which can help to optimize and narrow the range of the experimental conditions and to predict important characteristics of membrane formation by immersion precipitation method [1-8].

Flory Huggins theory is the basis for different models in literature [xiv-xv]. The model final result is an equation for the Gibbs free energy change due to polymer and solvent mixing [xvi-xvii]. The model proposed in our study, is a Flory-Huggins theory based model [2-8]. The model is developed to study the coagulation process over wide range of experimental conditions including temperature, volume fraction, and reaction time. The model takes into account the effect of volume fraction of each polymer, diffusion, the variation of the initial film thickness, and the coagulation bath temperature. This work aims to discuss the basis of solubility parameters, and their use in predicting polymer dissolution for polymer/solvent blends. It describes the thermodynamic model equations. Also, the model is used to illustrate the casting process for the ternary system comprising [polyamide-6 (PA-6), Chitosan (CS), and formic acid (FA)].

Thermodynamic Model of Polymer blend

Model description

The membrane preparation using the asymmetric polymer-polymer-solvent ternary blend is considered isothermal and controlled by diffusion. However, the model integrates a coupling between mass and heat transfer. The temperature is assumed uniform along the polymer film thickness. The Flory-Huggins interaction parameter, χ , denotes the immiscibility of different components in the blend. To induce the phase separation, the χ values of the two polymers have to be selected so that there is a free energy barrier between the immiscible polymer pairs. The Flory-Huggins interaction parameter X_{ij} is a function of temperature (T); the mole fraction of each polymer, and the degree of polymerization. In a ternary phase separation the critical value of the interaction parameter for spinodal decomposition to occur between two polymers is calculated from Equation (1).

$$X_{ij} = \frac{V_r(\delta_i - \delta_j)^2}{RT} \quad (1)$$

Where,

$$g_{ij} = \frac{(\delta_i - \delta_j)^2}{RT} \quad (2)$$

δ_i : Solubility parameter of component i, $\text{kJ}^{1/2} / \text{m}^{3/2}$

V_r : Reference volume which was chosen to be $100 \text{ cm}^3/\text{mol}$

The blend miscibility is assumed to decrease with increasing χ_{ij} . In the Flory-Huggins model, the interaction parameter, χ_{ij} , was considered independent of temperature and composition. In this work, the Flory-Huggins model was modified to use concentration and temperature dependent interaction parameters g_{ij} [3-5].

Effect of polymer blend composition

The effect of polymer composition was studied by varying the volume fractions of PA-6 and CS dissolved in formic acid (FA). The phase behavior of polymer blend can be described by the Gibbs free energy of mixing (ΔG_{mix}) by Equation (3), which is dependent on both the enthalpic (ΔH_{mix}) and entropic (ΔS_{mix}) changes of mixing [xviii-xix,xx].

$$\Delta G_m = \Delta H_m - T\Delta S_m \quad (3)$$

The mixture is stable over a certain composition range and the mixing process will occur spontaneously, when the change of Gibbs free energy shows a negative value[14,15]. The change in Gibbs free energy was studied for different temperatures to indicate the best mixing point.

The general expression of the extended Flory-Huggins model for ternary polymer solutions is shown in Equation (4):

$$\frac{\Delta G_m}{RT} = n_1 \ln \phi_1 + n_2 \ln \phi_2 + n_3 \ln \phi_3 + \bar{v}_1 n_1 \phi_2 g_{12} + \bar{v}_1 n_1 \phi_3 g_{13} + \bar{v}_2 n_2 \phi_3 g_{23} \quad (4)$$

Where; \bar{v}_i : Molar volume of component i, m^3/mol

Chemical potential, of components: 1-(PA), 2-(CS) and 3-solvent (FA), was used for calculating the ternary coexistence curve. Chemical potential was calculated taking the first derivative of the Gibbs free energy of mixing equation with respect to the mole fraction of each component, Equations 5, 6 and 7.

$$\frac{\Delta \mu_1}{v_1 RT} = \frac{\ln \phi_1}{v_1} - \frac{\phi_1}{v_1} - \frac{\phi_2}{v_2} - \frac{\phi_3}{v_3} + \frac{1}{v_1} + (g_{12} \phi_2 + g_{13} \phi_3)(1 - \phi_1) - g_{23} \phi_2 \phi_3 - g'_{12} \phi_2 \quad (5)$$

$$\frac{\Delta \mu_2}{v_2 RT} = \frac{\ln \phi_2}{v_2} - \frac{\phi_1}{v_1} - \frac{\phi_2}{v_2} - \frac{\phi_3}{v_3} + \frac{1}{v_2} + (g_{12} \phi_1 + g_{23} \phi_3)(1 - \phi_2) - g_{13} \phi_1 \phi_3 - g'_{23} \phi_3 \quad (6)$$

$$\frac{\Delta \mu_3}{v_3 RT} = \frac{\ln \phi_3}{v_3} - \frac{\phi_1}{v_1} - \frac{\phi_2}{v_2} - \frac{\phi_3}{v_3} + \frac{1}{v_3} + (g_{13} \phi_1 + g_{23} \phi_2)(1 - \phi_3) - g_{12} \phi_1 \phi_2 - g'_{23} \phi_2 \quad (7)$$

Equations 8 and 9 calculate the independent factor of the Flory-Huggins model g'_{ij} . The pseudo-binary compositions are expressed in a different notation as in Equations 10 and 11 [17-18,xxi-xxii].

$$g'_{12} = u_2(1 - u_2) \frac{dg_{12}}{du_2} \quad (8)$$

$$g'_{23} = v_2(1 - v_2) \frac{dg_{23}}{dv_2} \quad (9)$$

$$u_2 = \frac{\phi_i}{\phi_i + \phi_1} \quad (10)$$

$$v_2 = \frac{\phi_i}{\phi_i + \phi_2} \quad (11)$$

Where:

$\Delta\mu_i$: Change in chemical potential of component i, J/mol

ΔG_m : Change in Gibbs free energy of the mixture, J/mol

ϕ_i : Volume fraction of component i

n_i : Number of moles of component i, mole

Effect of polymer solution temperature

Temperature of polymers blend solution was varied (298, 333, 343, 353, and 363 K) to determine appropriate temperature of blend PA-6/CS polymer solution for preparation and to investigate the effect of solution temperature on the casted membrane specification.

The heat of mixing for any component can be calculated using Equation (12).

$$\Delta H_m = RT \chi_{ij} \phi_i (1 - \phi_i) \quad (12)$$

The critical temperature T_c value can be calculated from the Lyderson constants ($\sum \Delta_T$) and boiling point T_b at 1 atm using Equation (13).

$$T_c = \frac{T_b}{(0.567 + \sum \Delta_T - (\sum \Delta_T)^2)} \quad (13)$$

The cohesive energy and the cohesive energy density were calculated to determine the required energy for complete solubility [1-6, 17-18,xxiii]. Where, the cohesive energy, E ; of a material is defined as the increase in the internal energy per mole of the material if all of the intermolecular forces are eliminated. The cohesive energy density (CED) (Equation 14), is the energy required to break all intermolecular physical links in a unit volume of the material [17-20].

$$CED = \frac{E}{V} = \frac{\Delta H_v - RT}{V} \quad (14)$$

The solubility parameter δ is defined as the square root of the cohesive energy density as shown in Equation (15) [1, 17-20].

$$\delta = \sqrt{CED} \quad (15)$$

The molecular interactions and developed solubility parameters depend on three specific interactions, namely: non-polar interaction; polar cohesive forces and hydrogen bonding [15-19,xxiv]. Hildebrand solubility parameter can be determined by dividing the cohesive energy by the molar volume which provides the sum of the squares of the Hansen (δ_D), polar (δ_P), and hydrogen bonding dispersions (δ_H) components as shown by Equations (15) and (16).

$$\delta_t^2 = \delta_D^2 + \delta_p^2 + \delta_H^2 \quad (16)$$

Diffusion model of immersion precipitation

Diffusion model assumptions

Membrane preparation by immersion precipitation was investigated in several articles describing the diffusion models during membrane formation in coagulation bath [xxv - xxvi, xxvii-xxviii, xxix- xxx]. In our study, the model was developed based on the following assumptions:

1. The reference system is chosen centered around the interface between coagulation bath and polymer film.
2. The interface of the casted blend membrane in the coagulation bath has an initial composition similar to the original coagulation bath (distilled water).
3. The polymers blend can be regarded as a matrix phase in which the two other components diffuse.
4. The polymer solution doesn't form a closed system, and the volume of the polymer solution is not constant.
5. According to diffusion path of solvent from polymer film and until the spinodal is reached, one phase system is assumed.
6. The mobility of the polymer is much slower compared to the low molecular weight components.
7. The concentration of components in the coagulation bath depends on the diffusion coefficients.
8. The fluxes are independent of the film thickness.
9. Compositions at different points in the film at one instant of time can be represented by the so-called composition path

The immersion process is schematically represented by Figure 1. The entire process is governed by diffusion over polymer matrix and coagulation bath interface. A coordinate transformation from a Cartesian reference system (x) to a polymer fixed reference system (m) can circumvent the volume of polymer change consequences [xxxi, 13]. Cartesian coordinate (x) in the polymer solution is transformed in a polymer fixed reference system (m) and a reference system originating from the interface between polymer solution and coagulation bath (y). The transformation is given by Equations (17) and (18):

$$m = \int_0^L \phi_i dx \quad (17)$$

$$y = x - \Delta x \quad (18)$$

Where;

L: Total film thickness, m

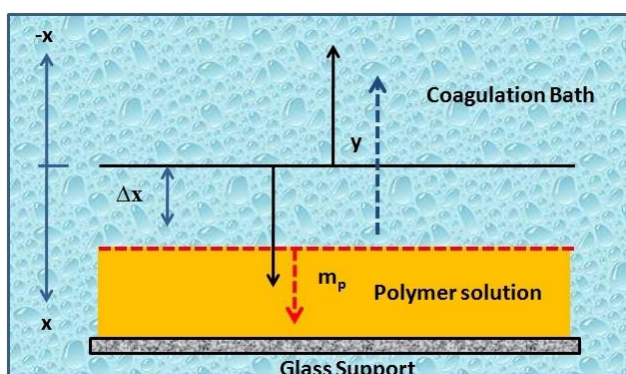


Figure 1: Schematic representation of the reference system to represent diffusion in the immersion precipitation process.

The formula which describes diffusion in the polymer solution is given in Equation (19). Where, component (i) represents polymer components (PA-6 and CS).

$$\frac{d(\phi_i)}{dt} = \bar{v}_i \frac{\partial}{\partial m} \left\{ \sum_{j=1:n-1} \phi_n L_{ij} \frac{\partial \mu_j}{\partial m} \right\} \quad (19)$$

Equation (20) represents the diffusion of solvent during immersion process in coagulation bath, where component (j) represents solvent (Formic acid, FA).

$$\frac{d\phi_i}{dt} = \bar{v}_i \frac{\partial}{\partial y} \left\{ \sum_{j=1:n-1} L'_{ij} \frac{\partial \mu_j}{\partial y} \right\} - \frac{\partial \phi_i}{\partial y} \sum_{k=1:n-1} J_k \quad (20)$$

Where:

$$i = 1:n - 1$$

t : Time, s

\bar{v}_i : Molar volume of component i, m³/mol

J_k : Flux of species k into the coagulation bath at the interface between polymer solution and coagulation bath at (y=0)

L_{ij} and L'_{ij} are the matrix elements of the phenomenological coefficient matrix L and L' respectively. L and L' are the inverse of the friction coefficient matrix R and R' respectively [19,20]. The R and R' can be calculated according to the following equations:

$$R_{ii} = - \left(\sum_{k \neq i} c_k R_{ik} \frac{RT \sigma_i}{M_i D_{ik}} + c_n \frac{RT \sigma_i}{M_i D_{in}} \right) \quad (21)$$

$$R'_{ii} = - \sum_{k \neq i} c_k \frac{RT \sigma_i}{M_i D_{ik}} \quad (22)$$

$$R_{ij} = c_j \frac{RT \sigma_i}{M_i D_{ij}} \text{ for } i \neq j \quad (23)$$

$$R'_{ij} = c_j \frac{RT \sigma_i}{M_i D_{ij}} \text{ for } i \neq j \quad (24)$$

Where:

D_{ij} : Binary diffusion coefficient between i and j, m²/s

R : Universal gas constant, J/mol/K

T : Temperature, K

M_i : Molecular weight of component i, kg/kmole

Initial conditions:

The initial conditions for the polymer solutions and the coagulation bath are shown below, respectively:

$$\phi_i(m, t = 0) = \phi_{i, \text{Polymersolution}}^0 \text{ for } m \neq 0 \text{ and } i = 1:n - 1$$

$$\phi_i(y, t = 0) = \phi_{i, \text{Coagulationbath}}^0 \text{ for } y \neq 0 \text{ and } i = 1:n - 1$$

Boundary conditions:

The boundary conditions for the polymer solutions and the coagulation bath are shown below, respectively:

$$\frac{d(\phi_i)}{dt} = 0 \quad \text{for } m = \infty$$

$$\frac{d(\phi_i)}{dt} = 0 \quad \text{for } y = \infty$$

Additional requirement is that the fluxes and chemical potentials of different components are equal at both sides of the interface:

$$\Delta\mu(m = 0) = \Delta\mu(y = 0) \text{ for } i = 1:n - 1$$

$$J_i(m = 0) = J_i(y = 0) \text{ for } i = 1:n - 1$$

RESULTS AND DISCUSSION

The model was employed to study the effect of coagulation conditions on the PA-6/CS blend membrane thermodynamic properties, and diffusion process on the polymer blend film formation in the coagulation bath as a function of the blend composition. The results are presented and discussed below in detail.

Model verification

Effect of polymer blend composition

The main phenomenon in membrane preparation is polymer dissolution, which consists of two transport processes solvent diffusion and chain disentanglement [xxxii, xxxiii-xxxiv]. The polymer gel formation takes place along two separate interfaces due to the polymer miscibility with the solvent, one of these interfaces is between the glassy polymer and the gel layer and the other interface originates between the gel layer and the solvent [1,7,xxxv]. This process is governed by the Gibbs free energy of mixing. However, a negative value of the free energy change means that the mixing process will occur spontaneously and according to Equation (2); the dissolution of a high molecular weight polymer is always associated with a slight positive entropy change. The enthalpy term is the crucial factor in determining the sign of the Gibbs free energy change. Also, the solubility parameters must be taken into account. Table 1 shows the numerical values of solubility parameters for Polyamide-6 (PA-6), Chitosan (CS), and formic acid [30,33,xxxvi].

Table 1: Solubility parameters of polymer solution components

Component	δ_d	δ_p	δ_h	$\Delta\delta$
PA-6	9.06	2.5	6	11.15
CS	2.6	2.14	3	4.5
FA	7	5.8	8.1	12.18

Effect of temperature was investigated and the Gibbs free energy of mixing and chemical potential of each component was calculated. Figure 2 and 3 show the change in Gibbs free energy and chemical potential of PA-6 as a result of varying the volume fraction of PA-6. Figures 2 and 3 show that the changes in Gibbs free energy of mixing and the chemical potential are always negative. The polymer blend is associated with a negative value of the change of free energy of mixing, $\Delta G_m \approx \Delta H_m \leq 0$ within the phase stability condition $(\beta^2 \Delta G_m / \beta^2 \phi) > 0$. Indicating that, the miscibility is not limited to two minimum compositions but the constant line. So, the phase separation will not occur during mixing of polymers (PA-6/CS) over all compositions [xxxvii, xxxviii].

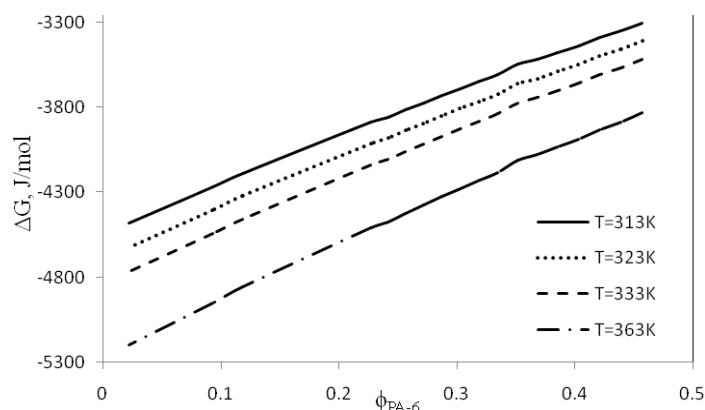


Figure 2: ΔG as a function of ϕ_{PA-6} at different temperatures

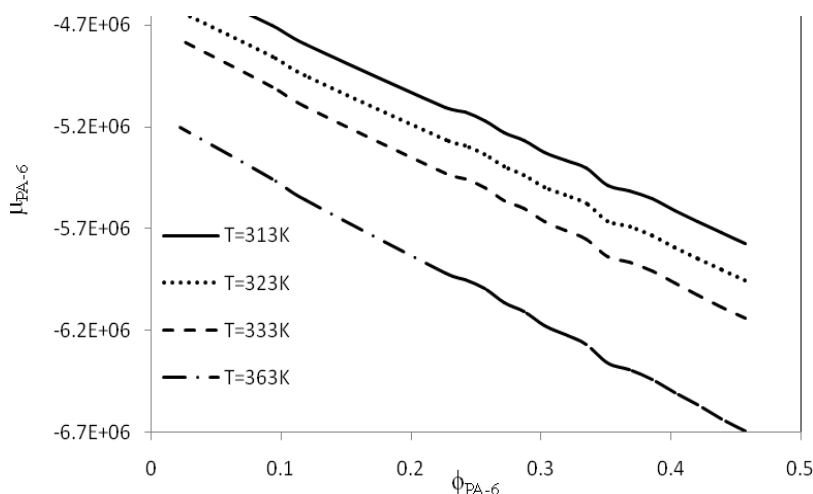


Figure 3: μ of PA-6 as a function of ϕ_{PA-6} at different temperatures

Critical temperatures of polymer blend solution

The critical point is defined mathematically as the point where the second and third derivatives of the Gibbs free energy with respect to the polymer volume fraction are zero. Figure 4 illustrates the interaction parameter of Flory-Huggins theory for PA-6/CS blend polymers versus temperature of solution. The interaction parameter showed inverse proportionality with temperature, the interaction parameter has increased from 0.0164 to 0.0178 as a result of decreasing the temperature from 323 to 298K. The UCST (Upper critical saturated temperature) behavior takes place when phase separation occurs upon cooling, where the g_{ij} interaction parameter decreases with increasing temperature as shown in Figure4.

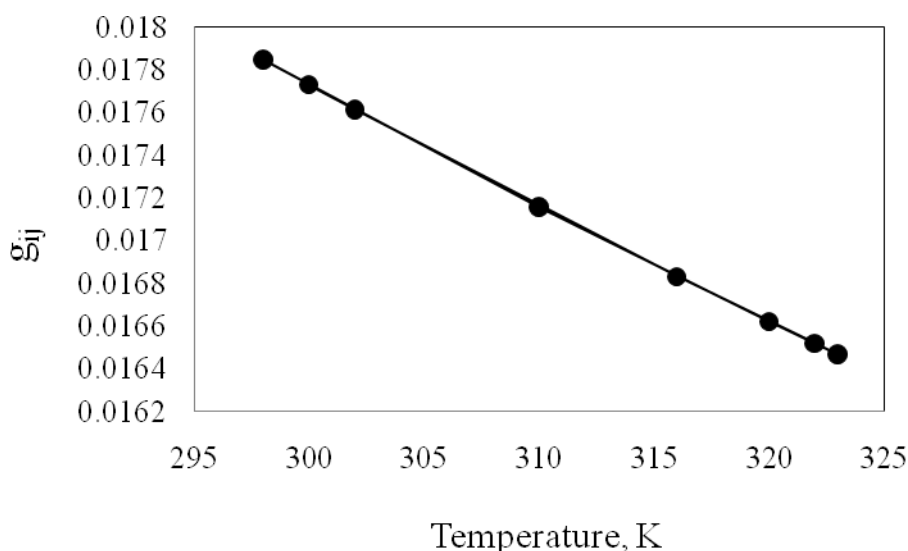


Figure 4: Interaction parameter of Flory-Huggins theory for PA-6/CS blend polymers versus temperature of polymer solution

Both UCST (Upper critical saturated temperature) and LCST (Lower critical saturated temperature) behaviors are observed in PA-6/CS polymers blend. Figure5showsthe UCST as a function ofthe volume fraction of polyamide (PA-6) polymer.The UCST is observed at323K andPA-6 volume fraction of 0.494. Figure 6showsthe LCST as a function of the volume fraction of Chitosan (CS). The LCST is observed at 344 K anda CS volume fraction of 0.116.From Figures 5 and 6, the interaction between two polymers PA-6 and CS will be

successful between 323-344 K. Further, LCST behavior suggests the existence of specific interactions between the polymers and the solvent.

The mixing of PA-6 and CS depends on reduction of combinatorial entropy upon mixing the two macromolecules together. The polymers blend mixture form a homogeneous phase at extreme temperatures or upon the addition of a solvent. Where in the case of PA-6/CS blend polymer, small molecules mixture and polymer gel layer undergo phase separation primarily upon cooling through an upper critical solution transition (UCST) 323K as shown in Figure 5. In some instances, the macromolecular mixture undergoes through a phase separation upon heating through a lower critical solution transition (LCST) 344K as shown in Figure 6. So, the superiority properties for mixing solution can be obtained for PA-6/CS blend solution in the temperature range 323-344K [xxxix, xl, xli].

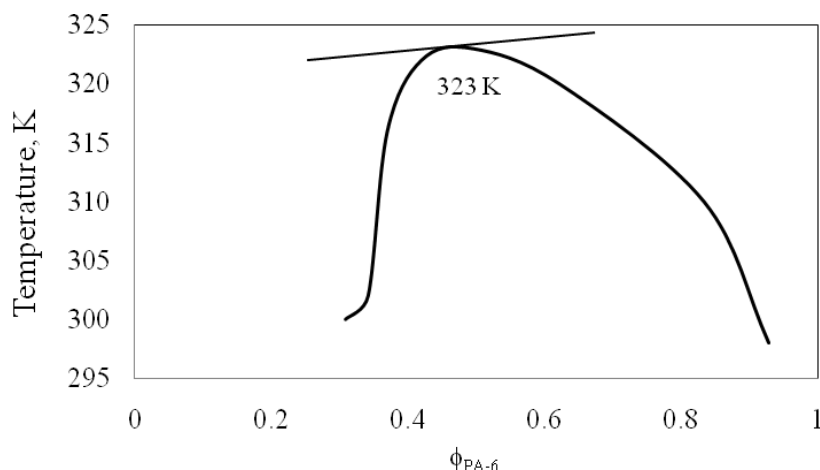


Figure 5: Upper critical solution temperature versus volume fraction of PA-6

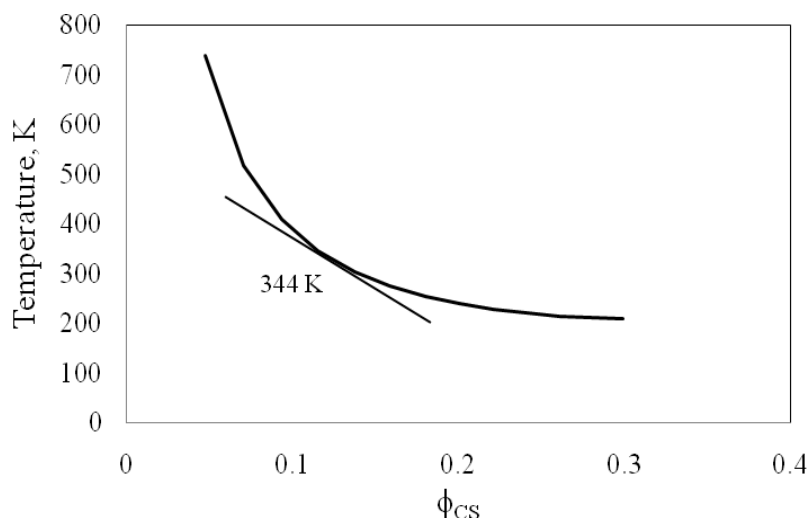


Figure 6: Lower critical solution temperature versus volume fraction of CS

Diffusion model solution of immersion precipitation

The immersion process is described by Equations 17-20. The immersion/precipitation time in the coagulation bath is related to the solvent dissolution from polymer solution to the coagulation bath. Increasing the solvent concentration in coagulation bath during immersion precipitation process indicates the phase separation process. Consequently, a polymer blend with high polymer concentration is produced which forms a

film of blend membrane [32-38]. Figure 7 illustrates the change in the ratio of volume fraction of polymer to volume fraction of solvent as a function of time throughout the membrane thickness. The ratio of volume fraction of polymer to volume fraction of solvent increased gradually until the coagulation time reached 500 min. Then the ratio of volume fractions increased slightly faster until the coagulation times was around 1000 min. Then the ratio of volume fractions shows a sharp rise. Figure 8 shows the change in volume fractions of CS and PA-6 as a function of time in the coagulation bath. A sharp drop is observed during the first 100 min owing to the precipitation process, and then a slow decrease of the polymers volume fractions is observed.

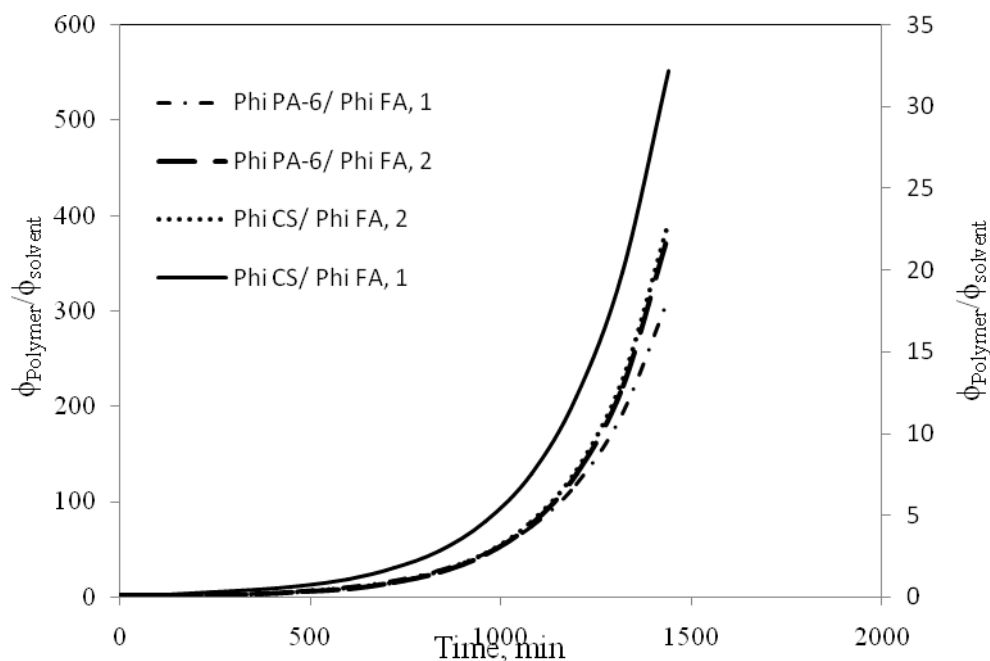


Figure 7: $\phi_{\text{polymer}}/\phi_{\text{solvent}}$ as a function of time, the dashed/dotted lines are plotted against the primary Y-axis; the solid line is plotted against the secondary Y-axis

1:T=298K, Initially; $\phi_{\text{CS}}= 0.28$, $\phi_{\text{PA-6}}= 0.271$
 2:T=298K, Initially; $\phi_{\text{CS}}= 0.047$, $\phi_{\text{PA-6}}= 0.457$

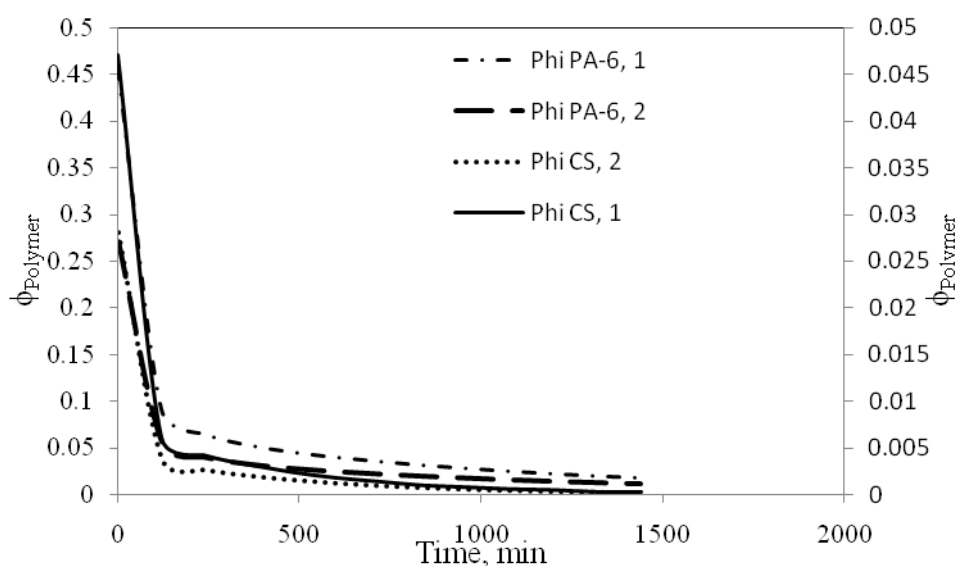


Figure 8: ϕ_{polymer} as a function of time in the coagulation bath, the solid line is plotted against the secondary Y-axis; the dashed/dotted lines are plotted against the primary Y-axis

- 1: T=298K, Initially; $\varphi_{CH} = 0.28$, $\varphi_{PA-6} = 0.271$
- 2: T=298K, Initially; $\varphi_{CH} = 0.047$, $\varphi_{PA-6} = 0.457$

Figure (7) indicates that the coagulation rate of membrane increases with time, where two initial polymer blend compositions were used; $\varphi_{CS} = 0.28$, $\varphi_{PA-6} = 0.271$ and $\varphi_{CS} = 0.047$, $\varphi_{PA-6} = 0.457$. The ratios of $\varphi_{PA-6}/\varphi_{FA}$ and $\varphi_{CS}/\varphi_{FA}$ increased due to coagulation process of membrane, while the polymer content is concentrated in the body of membrane and the solvent content outflows to the coagulation bath. However, using a composition of PA6 $\varphi_{PA-6} = 0.271$ and CS; $\varphi_{CS} = 0.28$ affected the membrane formation due to the higher coagulation rate of CS and lower coagulation rate of PA6. Using $\varphi_{PA-6} = 0.457$ and $\varphi_{CS} = 0.047$, the coagulation rate is dominated by PA6 coagulation leading to a better blend membrane with PA6 as a major component. When the membrane blend has higher CS than PA6 (for example $\varphi_{CS} = 0.59$ and $\varphi_{PA-6} = 0.022$), the coagulation rate is controlled by CS coagulation; yielding a better membrane compared to a membrane blend where CS and PA6 are mixed relatively similar volume fraction. Figure (8) indicates that the volume fraction of polymers in the coagulation bath (water) decreases sharply within the first 100 mins of coagulation. During membrane formation, the polymer concentration decreased in the bath. At the same time, the solvent concentration increased in the bath as a result of segregation of polymer material in the formed membrane.

Using initial conditions of $\varphi_{CS} = 0.28$, $\varphi_{PA-6} = 0.271$ at room temperature, Figures 9 and 10 show the ratio of $\varphi_{CS}/\varphi_{FA}$ and $\varphi_{PA-6}/\varphi_{FA}$ respectively as a function of time and membrane thickness in a 3D plot. The two figures have indicated a uniform distribution of PA-6 and CS across the membrane thickness. During the first 1000 mins the coagulation was proceeding gradually. After 1000 mins of coagulation, the ratio of $\varphi_{CS}/\varphi_{FA}$ and $\varphi_{PA-6}/\varphi_{FA}$ increased sharply indicating a faster coagulation. Figures (9) and (10) demonstrate that the thickness of polymers increased with time due to the membrane formation, where the thickness can reach to around 225 μm .

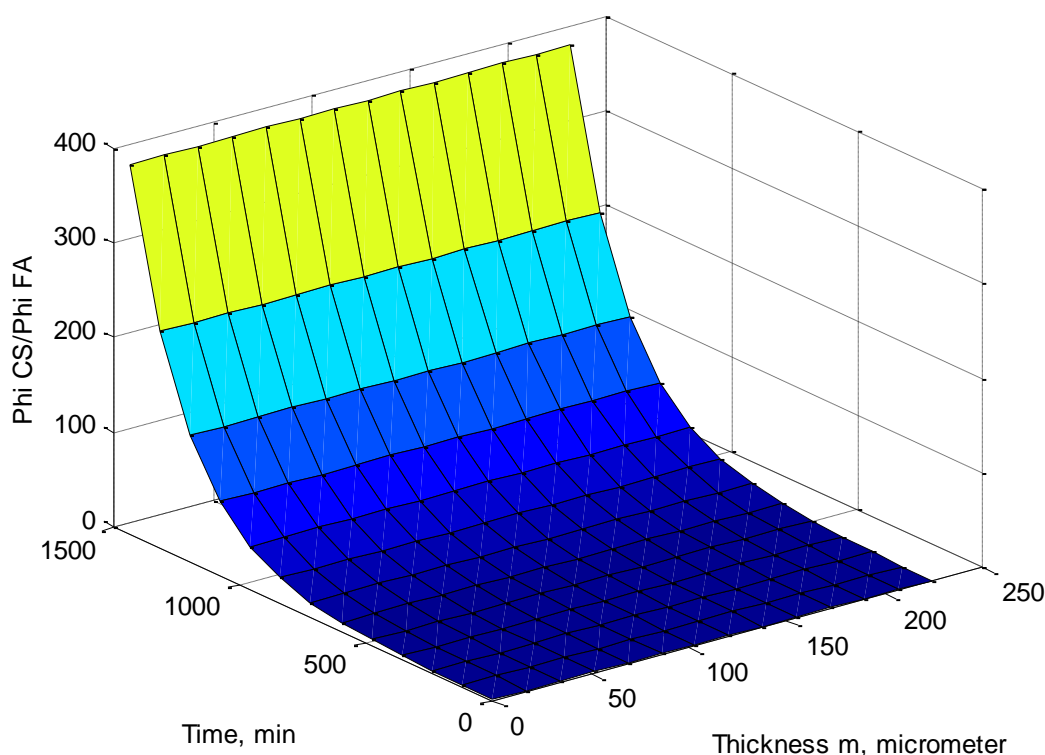


Figure 9: $\varphi_{CS}/\varphi_{FA}$ as a function of time and thickness of membrane at T=298K, Initially; $\varphi_{CS} = 0.28$, $\varphi_{PA-6} = 0.271$

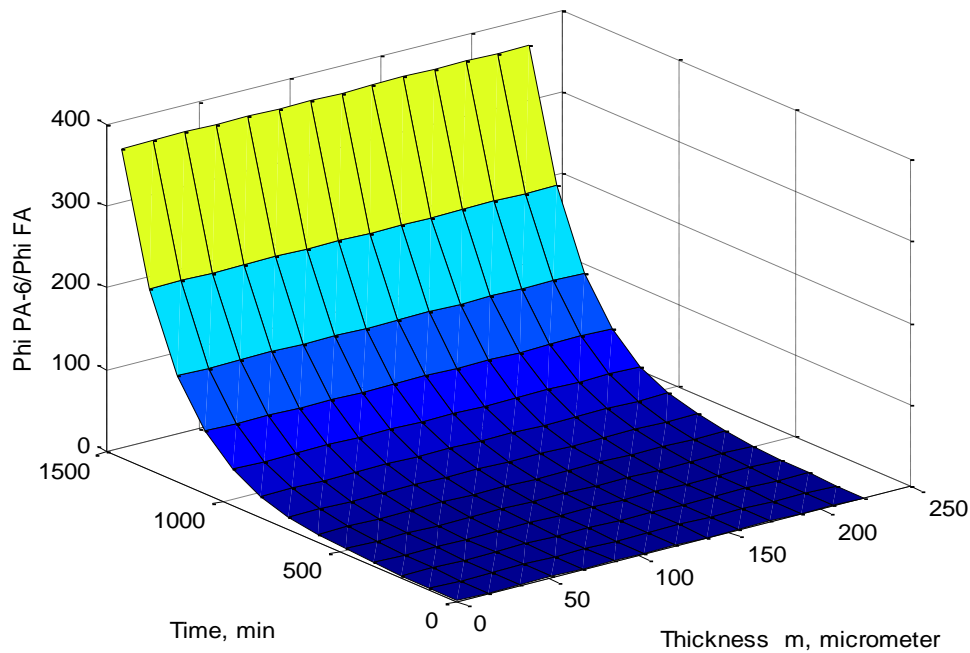


Figure 10: ϕ_{PA-6}/ϕ_{FA} as a function of time and thickness of membrane at $T=298K$, Initially; $\phi_{CS}= 0.28$, $\phi_{PA-6}= 0.271$

Figure 11 and 12 present ϕ_{CS} and ϕ_{PA-6} in the coagulation bath as a function of time and depth of the bath (40 cm), having the membrane/bath interface as a reference. The results show that once the membrane blend is placed in the coagulation bath; ϕ_{CS} and ϕ_{PA-6} increased sharply then starts to decline instantaneously owing to the precipitation of CS and PA-6 to form the membrane. The results indicated faster coagulation of CS compared to PA-6 as observed from Figure 7. Figures(11) and(12) show that the diffusion of polymer solution in the coagulation bath decreases with time. As CS and PA-6 precipitate on the membrane film, ϕ_{CS} and ϕ_{PA-6} decreased sharply in the bath accordingly CS and PA-6 precipitation rates will decrease further.

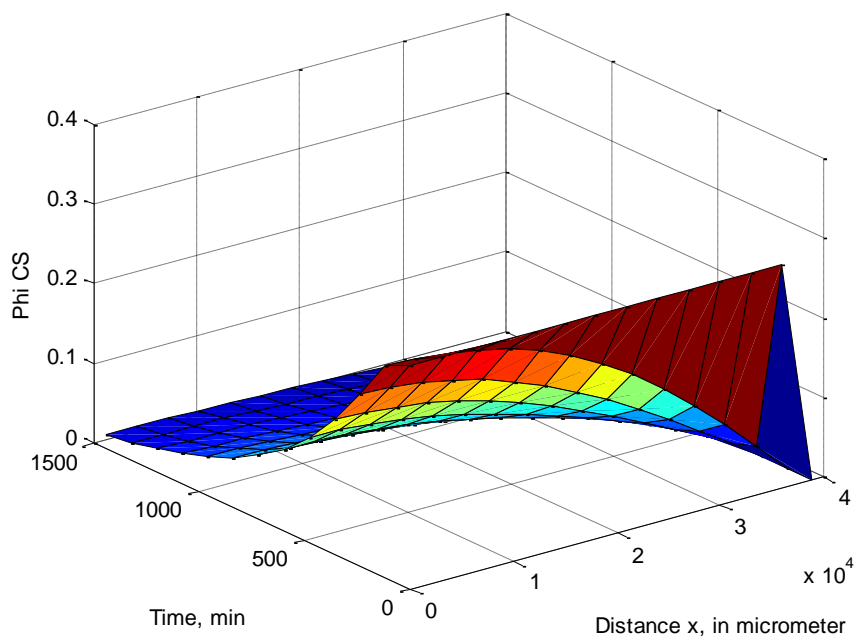


Figure 11: ϕ_{CS} as a function of time in the coagulation bath at $T=298K$, Initially; $\phi_{CS}= 0.28$, $\phi_{PA-6}= 0.271$

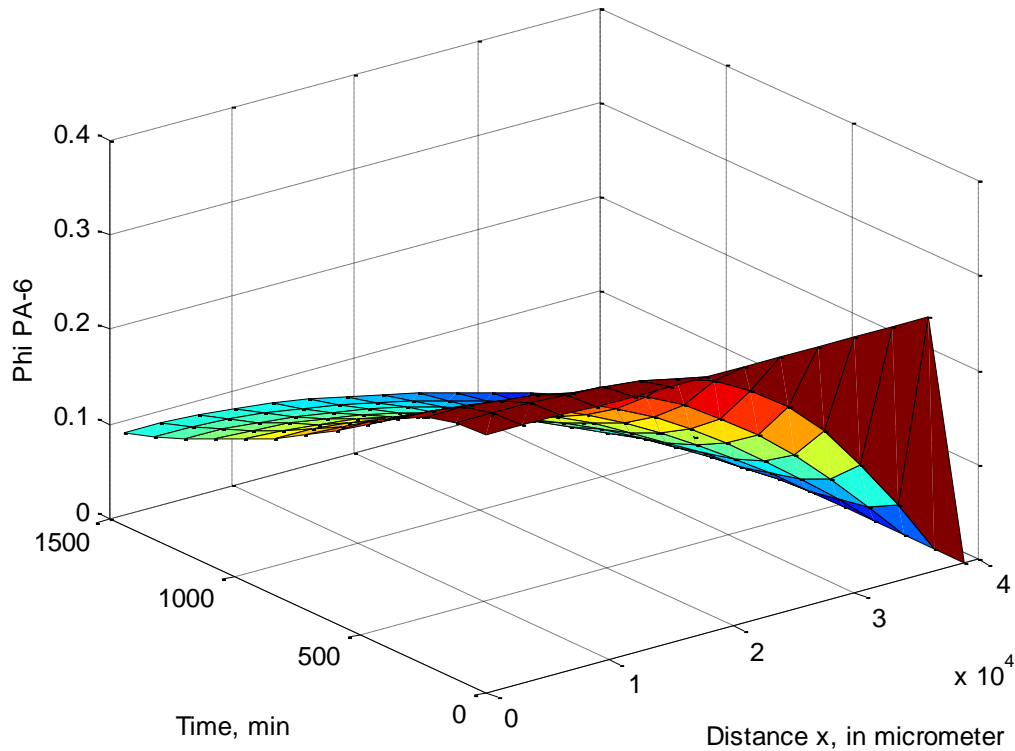


Figure 12: φ_{PA-6} as a function of time in the coagulation bath at $T=298K$, Initially; $\varphi_{CS}= 0.28$, $\varphi_{PA-6}= 0.271$

CONCLUSION

A mathematical model was developed to describe the behavior of PA-6/CS blend membrane preparation by phase inversion process. The following conclusions can be drawn from this study:

- The effect of polymer blend composition on the change of Gibbs free energy was always negative; the mixing was stable for all the polymers compositions at room temperature.
- The mathematical model explained the UCST and LCST behavior and indicated that the superiority properties of polymer solution was found in the critical temperature range between UCST 323 K and LCST 344 K, which can provide complete solubility.
- A diffusion model was developed to study the effect of immersion/ precipitation time in coagulation bath on the polymer blend formation. The model indicated that the solvent was segregating from polymer solution and dissolve in the coagulation bath during precipitation time. The volume fraction of solvent increased in the bath and the volume fraction of polymer decreased as a result of the membrane formation.
- The model predicts a better membrane formation when PA-6 or CS volume fraction is dominating in the blend due to the variation in the coagulation rate between the two polymers which may lead to membrane defects.
- The model expects the formation of a uniform membrane for all compositions with a membrane thickness around 225 μm .

ACKNOWLEDGMENT

This project was supported financially by the Science and Technology Development Fund (STDF), Egypt, Grant No 5019.

Nomenclature:

D_{ij} : Binary diffusion coefficient between i and j, m^2/s

ΔG : Gibbs free energy of mixing

J_k : Flux of species k into the coagulation bath at the interface between polymer solution and coagulation bath at ($y=0$)

L : Total film thickness, m

M_i : Molecular weight of component i, kg/kmol

R : Universal gas constant, J/mol/K

T : Temperature, K

t : Time, s

\bar{v}_i : Molar volume of component i, m^3/mol

Greek symbols:

$\Delta\mu_i$: Change in chemical potential of component i, J/mol

ϕ_i : Volume fraction of component i

n_i : Number of moles of component i, mole

δ_i : Solubility parameter, $kJ^{1/2}/m^{3/2}$

Subscripts:

PA-6: Polyamide-6

CS: Chitosan

FA: Formic acid

REFERENCES

- [1] M.H.V. Mulder, Basic principles of Membrane Technology. Kluwer Academic Publishers, Dordrecht, The Netherlands, 2000..
- [2] A. M. Bazargan, Z. Gholamvand, M. Naghavi, M. R. Shayegh and S. K. Sadrezaad, Phase Inversion Preparation and Morphological Study of Polyvinylidene Fluoride Ultrafiltration Membrane modified by Nano-Sized Alumina, Functional Materials Letters Vol. 2, No. 3 (2009) 113–119.
- [3] R.W. Baker, Membrane Technology and Applications, John Wiley & Sons, Ltd, West Sussex, England, 2004.
- [4] A. Ismail, L. Yean, Review on the Development of Defect-Free and Ultrathin- Skinned Asymmetric Membranes for Gas Separation through Manipulation of Phase Inversion and Rheological Factors, J. Appl. Polym. Sci. 88, 442–451 (2003).
- [5] P.J. Flory, Principles of Polymer Chemistry, Cornell University Press, Ithaca, NY, 1969.
- [6] A. Alkudhiri, N. Darwish, N. Hilal, Membrane distillation: a comprehensive review, Desalination 287 (2012) 2–18.
- [7] E. Drioli, L. Giorno, Membrane Operations: Innovative Separations and Transformations, Wiley-VCH, 2009.
- [8] M. Mulder, Basic Principles of Membrane Technology, Kluwer Academic Publishers, 1996.
- [9] I. Pinnau, B.D. Freeman, Formation and modification of polymeric membranes: overview, Membr. Form. Modif. 744 (2000) 1–22.
- [10] Ayman EL-GENDI, Heba Abdallah, Sahar Ali, Construction of Ternary Phase Diagram and Membrane Morphology Evaluation for Polyamide/Formic acid/Water System, Australian Journal of Basic and Applied Sciences, 6(5): 62-68, 2012 ISSN 1991-8178.
- [11] A. EL-Gendi, S.S. Ali, S.A. Ahmed and H.A. Talaat, Development of membrane blend using casting technique for water desalination, Membr. Wat. Treat. 3 (2012) 185-200.
- [12] A. Rawajefa, Polyamide based composite membrane, Part 1: preparation and characterization, Desalination 179 (2005) 265-272.
- [13] A. El-Gendi, H. Abdallah, Thermodynamic modeling of polyamide-6 (PA-6)/ cellulose acetate (CA) blend membrane prepared via casting technique, journal of polymer engineering, 2013 (8), page 701-712.
- [14] H. Abdallah, S. S. Ali, Thermodynamic modeling of PES/CA Blend Membrane Preparation, International Review of Chemical Engineering (I.RE.CH.E.), September, Vol. 4, N. 5, ISSN 2035-1755, 2012.
- [15] X. L. Wang, H. J. Qian, L. J. Chen, Z. Yuan Lu, Z. Sheng Li, Dissipative particle dynamics simulation on the polymer membrane formation by immersion precipitation, J. Membr. Sci. 311 (2008) 251–258.
- [16] S. A. Altinkaya, B. Ozbas, Modeling of asymmetric membrane formation by dry-casting method, J. Membr. Sci. 230 (2004) 71–89.

- [17] B. H. Chang, Y. Chan Bao, Molecular thermodynamics approach for liquid–liquid equilibria of the symmetric polymer blend systems, *Chem. Eng. Scie.* 58 (2003) 2931 – 2936..
- [18] B.A. Miller-Chou, J.L. Koenig, A review of polymer dissolution, *Prog.Polym. Sci.* 28 (2003) 1223–1270.
- [19] C. M Hansen, *Hansen solubility parameters: a user’s handbook*. Boca Raton, FL: CRC Press; 2000.
- [20] Miller-Chou BA, Koenig JL. *Prog.Polym. Sci.* 2003, 28, 1223 – 1270.
- [21] Yip Y, McHugh AJ. *J. Membr. Sci.* 2006, 271, 163 – 176.
- [22] Leea H, Krantz WB, Tak Hwang S. *J. Membr. Sci.* 2010, 354, 74 – 85.
- [23] S.S. Ali, H. Abdallah, Development of PES/CA Blend RO Membrane for Water Desalination, *International Review of Chemical Engineering (I.RE.CH.E.)*, Vol. 4, N. 3, ISSN 2035-1755, May 2012.
- [24] P. Menut, C. Pochat-Bohatier, A. Deratani, C. Dupuy, S. Guilbert, Structure formation of poly (ether-imide) films using non-solvent vapor induced phase separation: relationship between mass transfer and relative humidity, *Desalination* 145 (2002) 11–16.
- [25] H. Lee, W. B. Krantz, S. Tak Hwang, A model for wet-casting polymeric membranes incorporating nonequilibrium interfacial dynamics, vitrification and convection, *J. Membr. Sci*354 (2010) 74–85.
- [26] W. B. Krantz, A. R. Greenberg, D. J. Hellman, Dry-casting: Computer simulation, sensitivity analysis, experimental and phenomenological model studies *J. Membr. Sci*354 (2010) 178–188.
- [27] D. Bouyera, W. Werapuna, C. Pochat-Bohatiera, A. Deratani, Morphological properties of membranes fabricated by VIPS process using PEI/NMP/water system: SEM analysis and mass transfer modeling, *J. Membr. Sci* 349 (2010) 97–112.
- [28] X. L. Wang, H. J. Qian, L.J. Chen, Z.Yuan Lu, Z. Sheng Li, Dissipative particle dynamics simulation on the polymer membrane formation by immersion precipitation, *J. Membr. Sci* 311 (2008) 251–258.
- [29] X.He, C. Chen, Z. Jiang, Y. Su, Computer simulation of formation of polymeric ultrafiltration membrane via immersion precipitation, *J. Membr. Sci* 371 (2011) 108–116.
- [30] V.P. Khare , A.R. Greenberg , W.B. Krantz, Vapor-induced phase separation—effect of the humid air exposure step on membrane morphology Part I. Insights from mathematical modeling, *J. Membr. Sci* 258 (2005) 140–156.
- [31] G. A.Valerie and A. M. Mayes, A Simple Free Energy Model for Weakly Interacting Polymer Blends, *Macromolecules* 2001, 34, 1894-1907..
- [32] J. Min, M. Su, Performance analysis of a membrane-based energy recovery ventilator: Effects of membrane spacing and thickness on the ventilator performance, *Applied Thermal Engineering* 30 (2010) 991–997.
- [33] S. Velu, L. Muruganandam, Effect of phase inversion and rheological factor on formation of asymmetric polyethersulphoneultrafiltration membranes for separation of metal ions, *J. Chem. Bio. Phy. Sci. Sec. B*, Nov. 2011- Jan. 2012, Vol.2, No.1, 163-171.
- [34] N. Ghaemi, S.S. Madaeni, A. Alizadeh, P. Daraei ,V.Vatanpour , M. Falsafi, Fabrication of cellulose acetate/sodium dodecyl sulfate nanofiltration membrane: Characterization and performance in rejection of pesticides, *Desalination*, 290 (2012) 99–106.
- [35] K. Wa, D. Leea, P. K. Chanb, X. Feng, Morphology development and characterization of the phase-separated structure resulting from the thermal-induced phase separation phenomenon in polymer solutions under a temperature gradient, *Chem. Eng. Scie.* 59 (2004) 1491 – 1504.
- [36] B.M. Ganesh, A. M. Isloor, M. Padaki, Preparation and characterization of polysulfone and modified poly isobutylene-alt-maleic anhydride blend NF membrane, *Desalination*, 287 (2012) 103–108.
- [37] U.W. Gedde, *Polymer Physics*, Kluwer, Dordrecht, 1999.
- [38] A.A. Lefebvre, J.H. Lee, N.P. Balsara, B. Hammouda, “Fluctuations in Highly Metastable Polymer Blends”, *J. Polym.Sci., Polym.Phys.Ed.* 38, 1926-1930 (2000).
- [39] Y. Yip, A. J. McHugh, Modeling and simulation of nonsolvent vapor-induced phase separation, *J. Membr.Sci* 271 (2006) 163–176.
- [40] C. Hegde, A. M Isloor, M. Padaki, A. F. Ismail and L. W.J, New CPS-PPEES blend membranes for CaCl₂ and NaCl rejection, *Membr. Wat. Treat*, 3 (2012) 25-34.
- [41] I. C. Sanchez, R. H. Lacombe, *Statistical Thermodynamics of Polymer Solutions*, *Macromolecules*, 11 (1978) 6.